Design, Simulation, Fabrication, and Measurement of Silicon Photonics based Interferometers

Prabhat Narang
prabhatnarang.official@gmail.com

***Abstract*—The theory of Mach-Zehnder Interferometer (MZI) is discussed. MZI is then implemented in Lumerical Interconnect circuit. as well as in Klayout. Design is fabricated and measured. The results are compared between simulated and experimental values.**

***Index Terms*—Silicon-on-Insulator, Silicon Photonics, Michael Zehnder Interferometer**

I. Introduction

SILICON Photonics (SiPh) is a technology which leverages standard CMOS fabrication processes to create Photonic Integrated Circuits (PICs). In PICs, Silicon is used as an optical medium, and light can be guided and manipulated within the PICs to perform the desired tasks. In traditional CMOS Silicon ICs, electron flow is used to operate the 'Electrical' circuits which can be designed to do specific tasks like computation and numerical calculations for Artificial Intelligence. With SiPh as a field, there is a focus on shifting to 'Optical' circuits which can lead to faster and more energy-efficient devices.

II. Theory

A. Mach Zehnder Interferometer (MZI)

Mach Zehnder interferometer is an optical device whose output intensity is related to the relative phase shift accumulated by the light traveling in its two arms. The light in its two arms are derived from a single source, so that there is no initial phase difference. Let us say that $\beta_{1,2}, L_{1,2}, \alpha_{1,2}$ are the propagation constant, the length and the loss parameters, respectively, of waveguide 1 and 2, representing each arm of interferometer. Then the output intensity I_o of MZI is proportional to input intensity of light I_i:

$$I_o = \frac{1}{4} I_i \left| e^{-i\beta_1 L_1 - \frac{\alpha_1}{2} L_1} + e^{-i\beta_2 L_2 - \frac{\alpha_2}{2} L_2} \right|^2 \tag{1}$$

In an ideal case where waveguide is lossless ($\alpha_1 = \alpha_2 = 0$), the equation simplifies to:

$$I_o = \frac{1}{2} I_i \left(1 + \cos\left(\Delta(\beta L)\right)\right)^2 \tag{2}$$

We can assume that propagation constant β will not be too different for the two arms. Thus the equation becomes:

$$I_o = \frac{1}{2} I_i \left(1 + \cos\left(\beta \Delta L\right)\right)^2 \tag{3}$$

Thus, the output intensity varies with the difference in path length between the two arms (δ). The output intensity I_o is maximum when $\delta = n \cdot 2\pi, n = 0, 1, 2...$ and minimum when $\delta = n \cdot \pi, n = 1, 2, 3...$.

The minimum spacing in optical wavelength which causes maximum intensity peaks for a given ΔL is called Free Spectral Range (FSR) of interferometer. If λ_m, λ_{m+1} are the wavelength at which there is maximum intensity, then FSR is given by:

$$FSR(\lambda) = \lambda_{m+1} - \lambda_m \tag{4}$$

To find this value, the difference in δ for two wavelength must be minimum possible value, i.e. 2π ($\Delta\delta = 2\pi$). This gives the following relation for FSR:

$$FSR(\lambda) = \frac{\lambda^2}{\Delta L \cdot n_g} \tag{5}$$

where n_g is the group refractive index of the waveguide, given by

$$n_g = \left(n - \lambda \frac{dn}{d\lambda}\right) \tag{6}$$

TABLE I: n_{eff} for TE and TM fundamental modes

λ	Mode	n_{eff}
$1.55\mu m$	TE0	$2.433 + i1.243 \cdot 10^{-9}$
$1.55\mu m$	TM0	$1.779 + i8.786 \cdot 10^{-10}$

III. Modeling and Simulation

A. Waveguide

The waveguide geometry selected for this device is $t = 220nm$, $W = 500nm$. The waveguide is manufactured using Silicon-On-Insulator (SOI) fabrication process, which is compatible with CMOS fabrication techniques. Thickness $t = 220nm$ is of Silicon Oxide above the waver substrate, and is a standard in the industry. Width $W = 500nm$ is chosen because this waveguide supports only one mode as discussed later. The simulation is done using Lumerical Mode software.

Simulated mode profiles are given in Fig. 1, 2 for $\lambda = 1550nm$. The effective index (n_{eff}) corresponding to the modes is given in Table I. Loss (α) is related to the imaginary part of n_{eff}. For fundamental TE and TM modes, it is negligible and we can assume for short L, the waveguide will be lossless.

Wavelength sweep is done between $\lambda = 1500nm$ and $\lambda = 1600nm$ and waveguide is simulated for 10 points in between. We extract n_{eff} vs λ data points from the simulation for both TE and TM modes, and fit the data in second order Taylor expansion of n_{eff} about central wavelength $\lambda = 1500nm$ as:

$$n_{eff}(\lambda) = n_0 + n_1(\lambda - 1.55) - n_2(\lambda - 1.55)^2 \tag{7}$$

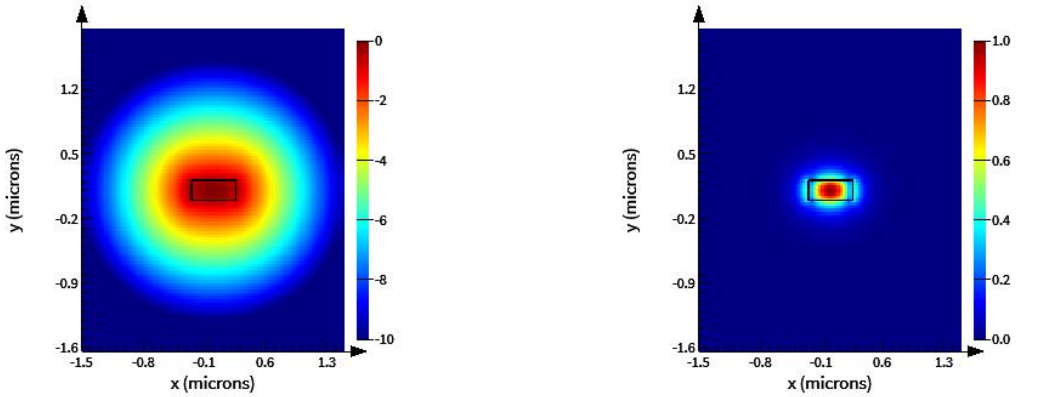

(a) (b)

Fig. 1: Simulated mode profile for fundamental TE mode (a) Electric field intensity $\left|\vec{E}\right|$ (b) Field component parallel to wafer and transverse to propagation direction E_x

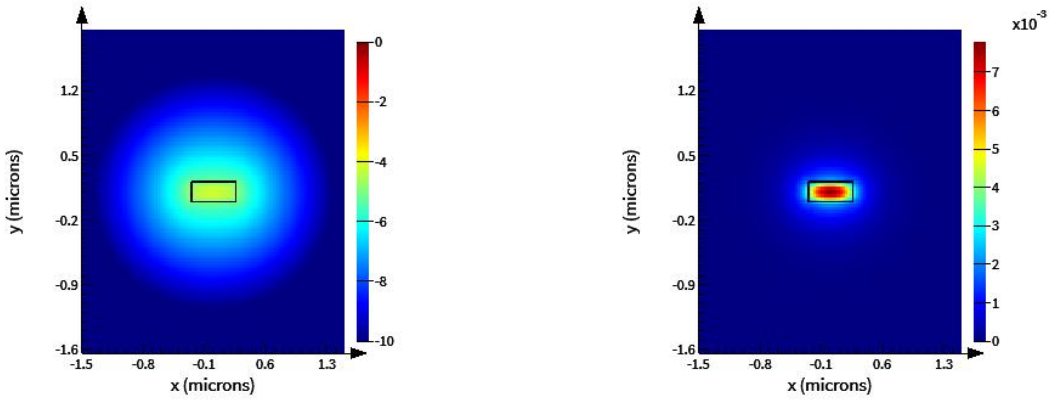

(a) (b)

Fig. 2: Simulated mode profile for fundamental TE mode (a) Magnetic field intensity $\left|\vec{H}\right|$ (b) Field component parallel to wafer and transverse to propagation direction H_x

This is called the compact model of waveguide. This model will be used in optical circuit simulation for the complete device. This simplifies and speeds up the simulation of optical circuits which can have many such individual waveguides as well as other passive components. The compact model for our waveguide for TE0 and TM0 modes is as follows

$$n_{eff,TE0}(\lambda) = 2.43361 - 1.13268(\lambda - 1.55) \\ -0.0429281(\lambda - 1.55)^2 \quad (8)$$

$$n_{eff,TM0}(\lambda) = 1.77923 - 1.30627(\lambda - 1.55) \\ +1.81862(\lambda - 1.55)^2 \quad (9)$$

B. Y Branch

Y branch is a multiport device that splits the input light intensity into half and sends to the output port. Ideal Y branch will reduce the input light intensity to half and send to output ports without any phase change. It is modeled and simulated in Lumerical Mode Software using the script *Ybranch_varFDTD_3DFDTD.lsf* provided in the course. The S matrix can be calculated from the simulation and can be used during optical circuit simulation. S matrix at $\lambda \approx 1.55\mu m$ extracted from simulated data by taking $\|S_{i,j}\|$ is given below:

$$S(\lambda \approx 1.55\mu m) = \begin{bmatrix} 0.0247 & 0.6943 & 0.6943 \\ 0.6952 & 0.0252 & 0.0147 \\ 0.6952 & 0.0147 & 0.0252 \end{bmatrix}$$

Since Y branch is a standard component of provided PDK and is experimentally characterized, we can use the model generated from the experimental data in PDK to simulate the optical circuit.

C. MZI

We can create an optical circuit using the models of waveguide, Y branch and Broadband Directional Coupler by

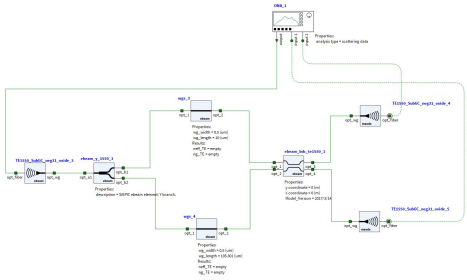

Fig. 3: Simulation results for the network.

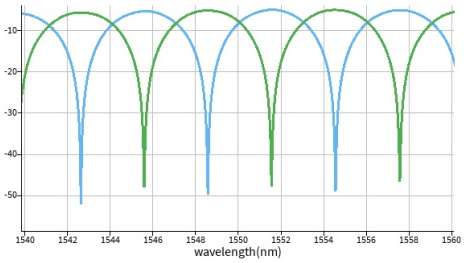

Fig. 4: Simulation results for the network.

connecting them together as in Fig. 3. Lumerical Interconnect software is used to simulate this circuit. Path length of one of the arms can be changed by changing the length parameter. Wavelength sweep simulation is performed which gives the graph in Fig. 4. From this graph, we can calculate FSR parameter. FSR comes out to be about 6 nm, which is what we get from equation 5 for $\Delta L \approx 95nm$, $n_g \approx 4.2$ and $\lambda = 1.55\mu m$.

IV. Layout

Layout for MZI is designed on KLayout tool. SiEPIC EBeam PDK and package are installed first. PDK gives the Layer stack information and other details related to fabrication. It also gives extensively simulated and experimentally verified device models that can be used for simulation. MZI designed using KLayout is shown in Fig. 5. Fig. 6 shows the simulation results after the KLayout design is converted to a netlist and simulated using Lumerical Interconnect. The scripts to do that are integrated within SiEPIC package for KLayout.

V. Fabrication

The photonic devices were fabricated using the NanoSOI MPW fabrication process by Applied Nanotools Inc. (http://www.appliednt.com/nanosoi; Edmonton, Canada) which is based on direct-write 100 keV electron beam lithography technology. Silicon-on-insulator wafers of 200 mm diameter, 220 nm device thickness and 2 µm buffer oxide thickness are used as the base material for the fabrication. The wafer was pre-diced into square substrates with dimensions of 25x25 mm, and lines were scribed into the substrate backsides to facilitate easy separation into smaller chips once fabrication was complete. After an initial wafer clean using piranha solution (3:1 H2SO4:H2O2) for 15 minutes and water/IPA rinse, hydrogen silsesquioxane (HSQ) resist was

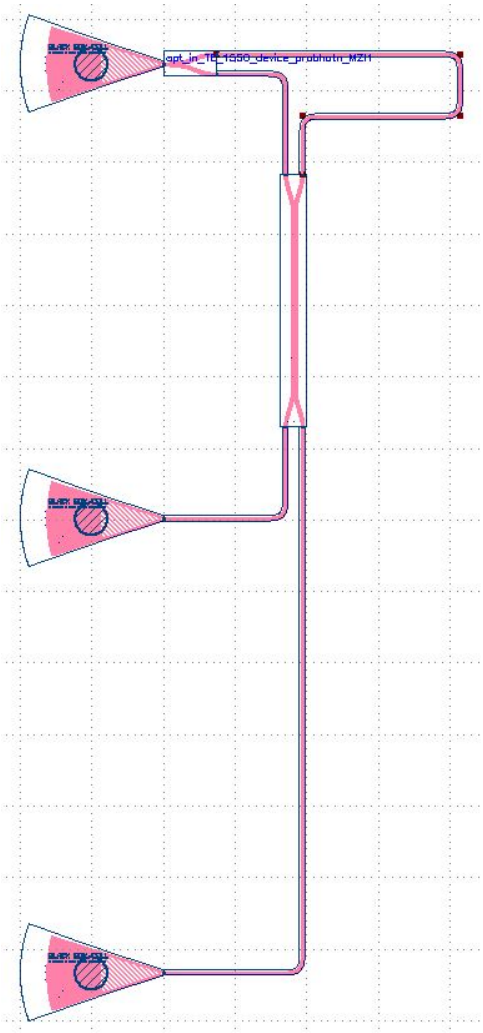

Fig. 5: Simulation results for the network.

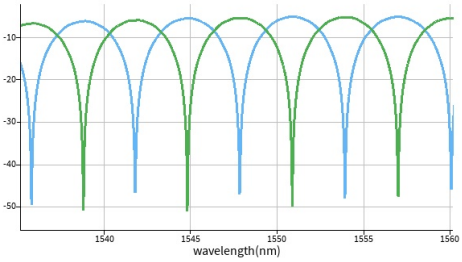

Fig. 6: Simulation results for the KLayout Design.

spin-coated onto the substrate and heated to evaporate the solvent. The photonic devices were patterned using a JEOL JBX-8100FS electron beam instrument at The University of British Columbia. The exposure dosage of the design was corrected for proximity effects that result from the backscatter of electrons from exposure of nearby features. Shape writing order was optimized for efficient patterning and minimal beam drift. After the e-beam exposure and subsequent development with a tetramethylammonium sulfate (TMAH) solution, the devices were inspected optically for residues

and/or defects. The chips were then mounted on a 4” handle wafer and underwent an anisotropic ICP-RIE etch process using chlorine after qualification of the etch rate. The resist was removed from the surface of the devices using a 10:1 buffer oxide wet etch, and the devices were inspected using a scanning electron microscope (SEM) to verify patterning and etch quality. A 2.2 µm oxide cladding was deposited using a plasma-enhanced chemical vapour deposition (PECVD) process based on tetraethyl orthosilicate (TEOS) at 300ºC. Reflectrometry measurements were performed throughout the process to verify the device layer, buffer oxide and cladding thicknesses before delivery.

VI. Measurement Description

To characterize the devices, a custom-built automated test setup [2, 6] with automated control software written in Python was used [3]. An Agilent 81600B tunable laser was used as the input source and Agilent 81635A optical power sensors as the output detectors. The wavelength was swept from 1500 to 1600 nm in 10 pm steps. A polarization maintaining (PM) fibre was used to maintain the polarization state of the light, to couple the TE polarization into the grating couplers [4]. A 90° rotation was used to inject light into the TM grating couplers [4]. A polarization maintaining fibre array was used to couple light in/out of the chip [5].

VII. Experimental Data Analysis

Data measured from the silicon device is shown in Fig. 7. The data is noisy near the edge of the measurement range. We limit the wavelength range to remove the noise as shown in Fig. 8. The experimentally measured data is plotted with the corresponding simulated data for the same port in Fig. 9. The data match very closely with the simulation. If we look closely at the center of the graph, the peaks from simulation match the peaks in the experimental data. But in the left and right side of the graph, the simulated peaks seem to be present right and left side of the experimental peak respectively. This is due to slight variation of group index (n_g) with wavelength (dispersion).

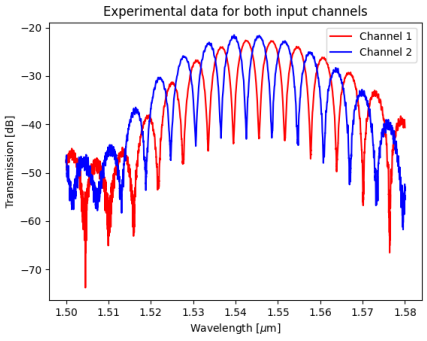

Fig. 7: Measured Data

Ideally, simulation data should match perfectly with experimental data. But fabrication has inherent variation and exact width and height we simulate for cannot be achieved

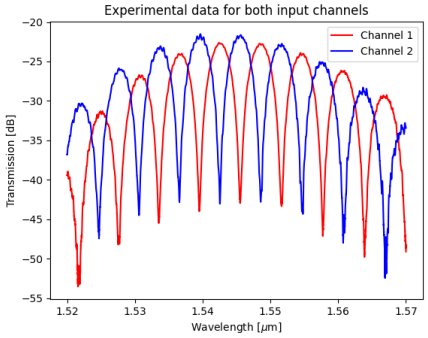

Fig. 8: Measured Data with noisy part removed

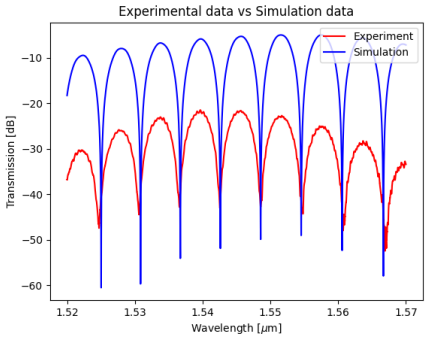

Fig. 9: Measurement vs Simulation

practically. Instead, we can get a range of height and width of waveguide within which the waveguide can be fabricated. This data is gathered over numerous test fabrication and is part of the PDK delivered by the manufacturer. Since we have this range of variations, we can simulate the waveguide at extreme cases of height and width and are called ’corners’. The fabricated device should be within these limits.

Borrowing the terminology from semiconductor manufacturing, each corner was named and has corresponding height and width values. Lumerical mode script was written to go over all the corners and simulate waveguide according to each corner’s dimensions. Waveguide parameters like n_{eff}, n_g were extracted from simulation for each corner. Variation of effective index for all the corners is shown in Fig. 10. Range of n_{eff} (10), n_g values (11) and corresponding FSR values calculated (12) at $\lambda = 1.55\mu m$ is given.

$$n_{eff}(\lambda = 1.55\mu m) = \{2.361, 2.465\} \tag{10}$$

$$n_g(\lambda = 1.55\mu m) = \{4.161, 4.244\} \tag{11}$$

$$FSR(\lambda = 1.55\mu m)(nm) = \{5.942, 6.060\} \tag{12}$$

Compact model and Interconnect model (*.ldf) of waveguide was generated for each corner.

Waveguide models from EBeam SiEPIC PDK used in Interconnect circuit were replaced with Interconnect models from MODE simulation. Lumerical Interconnect script was written to go over all the corners and simulate the device by using corresponding model for that corner. FSR is extracted

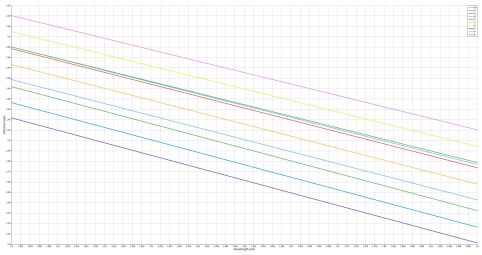

Fig. 10: Effective Index vs Wavelength for all Corners

from simulation by taking a mean of FSR values near target wavelength $\lambda = 1.55\mu m \pm \Delta\lambda$ as shown in Fig. 11. This averaging algorithm needs to be improved, as it does not give proper results. Range of simulated FSR values (13) across all corners is given.

$$FSR(\lambda \approx 1.55\mu m)(nm) = \{5.9267, 6.0302\} \tag{13}$$

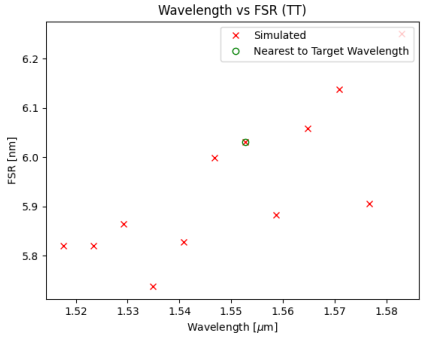

Fig. 11: Simulated FSR vales for corner TT

Device and waveguide parameters are extracted from experimental data using python script from Huixu (Chandler) Deng (Fig. 12). Following are the parameters extracted.

$$\begin{aligned} n_{eff}(\lambda) = 2.40326976 - 1.12195018(\lambda - 1.55) \\ -0.47990233(\lambda - 1.55)^2 \end{aligned} \tag{14}$$

$$FSR = 6.0299nm \tag{15}$$

$$n_g(\lambda = 1.55\mu m) = 4.142 \tag{16}$$

$$Dispersion[ps/nm/km] = -4962.424 \tag{17}$$

TABLE II: Parameters for all corners

Corner	Dim	n_{eff}	n_g	Calc FSR
NN	220.0x500.0	2.433	4.189	6.020
FS	223.1x470.0	2.392	4.244	5.942
TS	223.1x490.0	2.431	4.210	5.990
SS	223.1x510.0	2.465	4.172	6.044
FT	219.2x470.0	2.376	4.236	5.953
TT	219.2x490.0	2.415	4.203	6.000
ST	219.2x510.0	2.449	4.166	6.053
FF	215.3x470.0	2.361	4.230	5.961
TF	215.3x490.0	2.400	4.197	6.008
SF	215.3x510.0	2.434	4.161	6.060

Diagram describing each corner in terms of variation in waveguide geometry is given in Fig. 13. The results are tabulated for all corners and given in Table II.

VIII. Conclusion

The waveguide parameters such as the values of n_{eff}, n_g and the device parameter FSR were extracted from the experimental data. The waveguide was simulated for all corner cases for waveguide width and height due to manufacturing variations. The waveguide parameters (n_{eff}, n_g) for all corner cases were tabulated. The waveguide model was generated from the previous simulations, and was used to simulate MZI device. All values of FSR corresponding to corner scenarios were tabulated along with the calculated FSR values. The experimental FSR values lie within the maximum and minimum possible values of FSR. Hence, we can conclude that our modeling and simulation of device match well with the fabricated device. Currently extracting FSR from Interconnect simulation has some issues and will be fixed in future.

IX. Acknowledgment

I acknowledge the edX UBCx Silicon Photonics Design, Fabrication and Data Analysis course. Special thanks to Professor Lukas Chrostowski for designing a well-structured course, answering our queries and providing guidance throughout the course. The devices were fabricated by Applied NanoTools (ANT). I acknowledge Ansys for providing with Lumerical Solutions license for this course, Mathworks, Mentor Graphics, Python, and KLayout for the design software.

References

[1] R. J. Bojko, J. Li, L. He, T. Baehr-Jones, M. Hochberg, and Y. Aida, "Electron beam lithography writing strategies for low loss, high confinement silicon optical waveguides," J. Vacuum Sci. Technol. B 29, 06F309 (2011)

[2] Lukas Chrostowski, Michael Hochberg, chapter 12 in "Silicon Photonics Design: From Devices to Systems", Cambridge University Press, 2015

[3] http://siepic.ubc.ca/probestation, using Python code developed by Michael Caverley.

[4] Yun Wang, Xu Wang, Jonas Flueckiger, Han Yun, Wei Shi, Richard Bojko, Nicolas A. F. Jaeger, Lukas Chrostowski, "Focusing sub-wavelength grating couplers with low back reflections for rapid prototyping of silicon photonic circuits", Optics Express Vol. 22, Issue 17, pp. 20652-20662 (2014) doi: 10.1364/OE.22.020652

[5] www.plcconnections.com, PLC Connections, Columbus OH, USA.

[6] http://mapleleafphotonics.com, Maple Leaf Photonics, Seattle WA, USA.

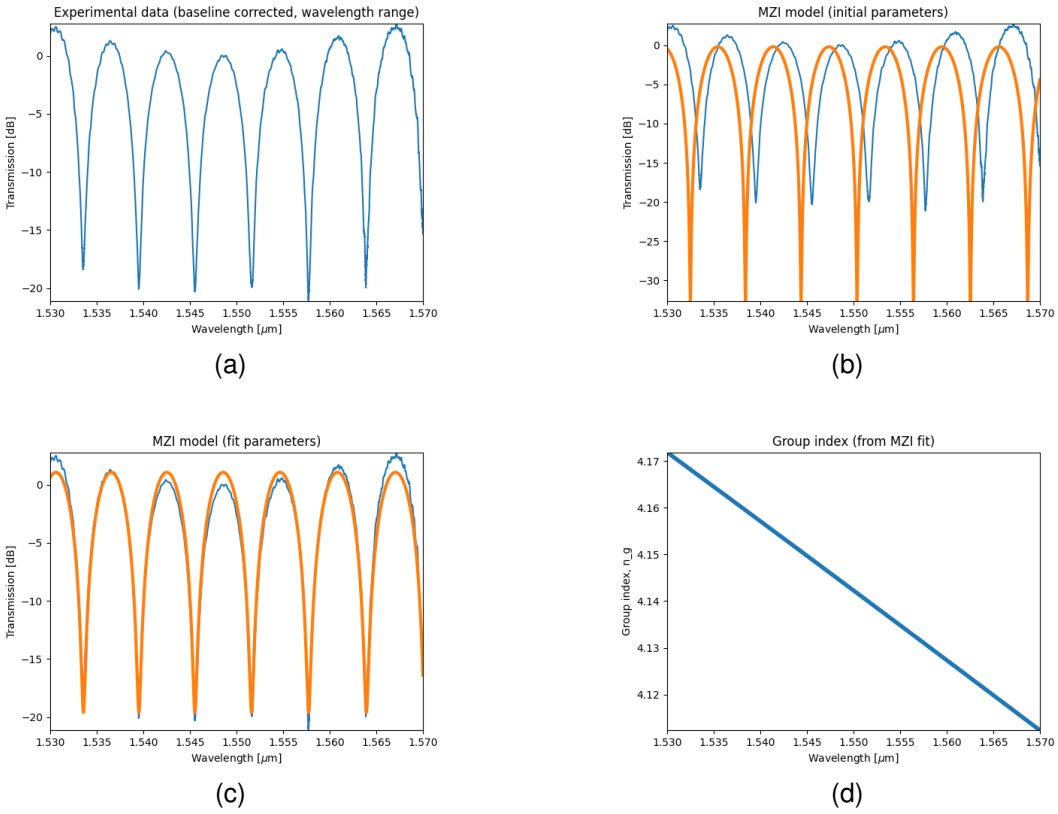

Fig. 12: Measured Data Fitting with Autocorrelation (a) Baseline correction (b) Initial Fit with MZI model (c) Fit with MZI Model on Measured Data (d) n_g vs λ

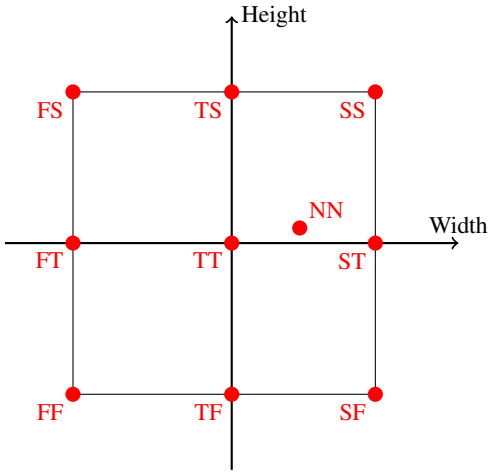

Fig. 13: Height vs Width of fabricated waveguide and corresponding corners